Why Are Lipid Rafts Not Observed In Vivo?

Arun Yethiraj and James C. Weisshaar
Department of Chemistry, University of Wisconsin, Madison, Wisconsin 53706

ABSTRACT The existence of lipid rafts in live cells remains a topic of lively debate. Although large, micrometer-sized rafts are readily observed in artificial membranes, attempts to observe analogous domains in live cells place an upper limit of ~5 nm on their size. We suggest that integral membrane proteins attached to the cytoskeleton act as obstacles that limit the size of lipid domains. Computer simulations of a binary lipid mixture show that the presence of protein obstacles at only 5–10% by area dramatically reduces the tendency of the lipids to phase separate. These calculations emphasize the importance of spatial heterogeneity in cell membranes, which limits the transferability of conclusions drawn from artificial membranes to live cells.

INTRODUCTION

Lipid rafts are segregated cholesterol-rich membrane domains whose distinct physical and chemical properties are believed to confer biological function (1–4). Lipid rafts have been postulated to be important in many diverse cellular processes, including bacterial and viral targeting of cells (5), insulin-stimulated glucose transport (6), T-cell receptor signaling (7), stabilization of microtubules (8), axon growth and guidance (9), cell apoptosis (10), and amyloid-β oligomerization (11). The very existence of rafts in live cells, however, is hotly debated, and direct evidence of rafts in vivo is sparse. Although large, micrometer-sized rafts are readily observed in artificial membranes (12), attempts to observe analogous domains in live cells place an upper limit of ~5 nm on their size (13).

Here we propose a new idea for why micrometer-sized rafts might not be present in cells: integral membrane proteins attached to the cytoskeleton act as immobile obstacles that limit the size of lipid domains. Using computer simulations of a lattice model of the membrane, we show that the presence of protein obstacles at only 5–10% by area dramatically reduces the tendency of the lipids to phase separate and suggest that immobile proteins might be important in the biophysics of membranes.

The existence of rafts was initially inferred from biochemical studies that consistently found a ''detergent-resistant membrane fraction'' rich in cholesterol (Chol) and glycosphingolipids as well as the glycosyl-phosphatidylinositol anchored proteins (GPI-APs) that play an important role in cell signaling (14,15). The ''raft hypothesis'' suggests that large domains, enriched in Chol, are formed, and these provide a mechanism for the concentration of GPI-APs, which is important for the amplification of signaling. There is no direct evidence for rafts, however, and it is common for processes that depend on Chol concentration to be declared to be raft-driven.

In an incisive recent experiment, Sharma et al. (13) carried out fluorescence resonant energy transfer measurements on labeled GPI-APs in live cells. Careful analysis showed that most of the GPI-APs exist as monomers, with a smaller fraction, ~20–40%, in small clusters of at most four proteins. Lipid rafts, if they exist at all, would contain only ~40 lipid molecules and may be highly transitory; perhaps they are better described as ''membrane nanodomains'' (2). These conclusions are consistent with most other recent experiments on live cells (4,16,17). Meanwhile, large, micrometer-diameter, phase-separated lipid domains are readily observed in artificial, protein-free lipid bilayers of composition similar to the detergent-resistant membrane fractions (18,19). This striking difference in phase behavior between biological membranes and synthetic membranes demands a physical explanation.

In this article we suggest a simple but powerful effect that might prevent formation of micrometer-sized rafts in live cells. We consider a lattice model with two lipid components, A and B, that tend to phase separate because of favorable A–A and B–B energetic interactions and calculate the phase diagram as a function of the area fraction of protein obstacles. We find that inert, immobile obstacles intended to model integral membrane proteins bound to the underlying cytoskeleton suppress the temperature at which phase separation occurs by a significant amount. These protein obstacles do not hinder the formation of smaller nanometer-sized lipid domains. These effects of protein obstacles are robust and must certainly be accounted for in any comprehensive physical model of lipid domain formation in biological membranes.

The next section describes the model and simulation method, and this is followed by a description and discussion of results. The final section summarizes our main conclusions.

Model and simulation method

We model the binary lipid mixture using an Ising model on a square lattice (Fig. 1), with nearest-neighbor attractive

Submitted January 10, 2007, and accepted for publication June 19, 2007.

Address reprint requests to Arun Yethiraj, Department of Chemistry, University of Wisconsin, Madison, WI 53706. E-mail: yethiraj@chem.wisc.edu.

Editor: Michael Edidin.

0006-3495/07/11/3113/07 $2.00

doi: 10.1529/biophysj.106.101931

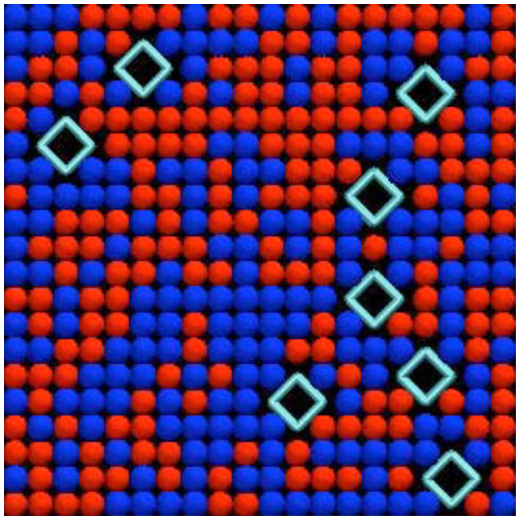

FIGURE 1 Picture of Ising model where diamonds represent membrane protein obstacles and blue and red squares the two lipid components A and B.

energy of $-\varepsilon$ between like pairs A–A and B–B and repulsive energy $+\varepsilon$ between unlike pairs A–B, i.e., $\varepsilon_{AA} = \varepsilon_{BB} = -\varepsilon$, and $\varepsilon_{AB} = +\varepsilon$. The Hamiltonian for the system is

$$H = \varepsilon \sum_{\langle ij \rangle} s_i s_j, \quad (1)$$

where i and j denote lattice sites, the sum is over nearest neighbors, and $s_i = 0$ if lattice site i belongs to an obstacle, $s_i = 1$ for species A, and $s_i = -1$ for species B. We choose ε so that the transition temperature from two separate liquid phases to a single, mixed phase mimics that of a canonical raft-forming lipid mixture in vitro. Experimentally, a 1:1:1 mixture of palmitoyl-sphingomyelin, dioleoylphosphatidylcholine, and Chol in giant unilamellar vesicles displays a liquid-liquid demixing phase transition at ~40°C (19). In the model, this temperature fixes $\varepsilon = 0.27$ kcal/mol, the only parameter characterizing the lipid mixture. The protein ''obstacles'' are modeled as noninteracting crosses that occupy five neighboring lattice sites (*diamonds* in Fig. 1). The simulation system consists of a square lattice of L^2 sites, with L in the range 20–150, with periodic boundary conditions in all directions. For $L = 50$, and assuming a single lipid diameter of ~0.7 nm, the lattice occupies only 35 nm × 35 nm; it is much smaller than a micrometer-sized raft. A fixed fraction ϕ of these sites is occupied by the protein obstacles, which are held static in space for each realization of the model.

One could incorporate an interaction between the obstacles and the lipid components, but as long as this interaction is the same for both components, it does not affect the phase diagram. This is because the primary move in the simulation is ''flipping a spin'' from +1 to −1 (or vice versa), with the move accepted according to the Metropolis criterion (20), i.e., with probability proportional to $\exp(-\beta\Delta H)$ where $\beta = 1/kT$, where k is Boltzmann's constant, T is the temperature, and ΔH is the change in energy caused by the move. If the lipid-obstacle interaction is the same for both components, it makes no contribution to ΔH and therefore does not affect the configurations sampled and hence the phase diagram.

The nature of the lattice is not expected to affect the results in a significant fashion. The qualitative features of phase diagrams are similar for lattice and off-lattice models (21), and the type of lattice, e.g., hexagonal or square, is not expected to be important. A hexagonal lattice has a higher coordination number than a square lattice and, for a given value of ε, will result in a higher critical temperature. Because we fit ε to experiment, in the absence of obstacles, the type of lattice will merely alter the value (in kcal/mol) of ε rather than the phase behavior itself. The nature of the lattice does, of course, influence the nature of the obstacles that can be incorporated.

The simulations proceed via a straightforward implementation of the Wolff cluster algorithm (22). This is a rejection-free algorithm where a cluster of molecules (''spins'') is first determined as follows. Consider two lattice sites i and j such that the energy of interaction between them is ε_{ij}. If $\varepsilon_{ij} < 0$, the two sites belong to the same cluster with probability $1 - \exp(-2\ \varepsilon_{ij}/kT)$. The clusters are identified using the Hoshen-Kopelman algorithm (23). Once a cluster has been found, the identity of all the molecules in the cluster is changed. It has been shown that this algorithm samples the correct ensemble and is very efficient because all moves are accepted. On the order of 10^6 such moves are carried out for each temperature and ϕ, and the required properties are averaged over the configurations generated. For a given temperature the simulation method samples all lipid compositions with appropriate statistical weight. The phase diagram is then obtained from the probability distribution function of the compositions, as described below.

In the binary mixture a phase separation (into coexisting A-rich and B-rich phases) occurs as the temperature is decreased. The goal of this work was to determine the two-phase coexistence boundary and critical temperature, T_c, as a function of the area fraction of the protein obstacles. We do this by calculating the probability distribution function, $P(x_A)$, of the mole fraction for various temperatures. At temperatures above the critical temperature, $P(x_A)$ peaks at $x_A = 1 - x_B = 0.5$ because, by symmetry, the chemical potentials of the two components are equal. For finite systems $P(x_A)$ is a broad bell-shaped curve, and as the system size is increased, $P(x_A)$ becomes sharper and is a δ function for infinite systems. For temperatures below the critical temperature, $P(x_A)$ shows two peaks. The behavior of $P(x_A)$ for a pure lipid mixture (no obstacles) is shown in Fig. 2 for various temperatures. At high temperature, the mixing entropy dominates the lipid-lipid attractive energy, the system becomes more randomly mixed, and the distribution narrows. As the temperature is lowered toward T_c, the peak in $P(x_A)$ gradually broadens. For temperatures below T_c, $P(x_A)$

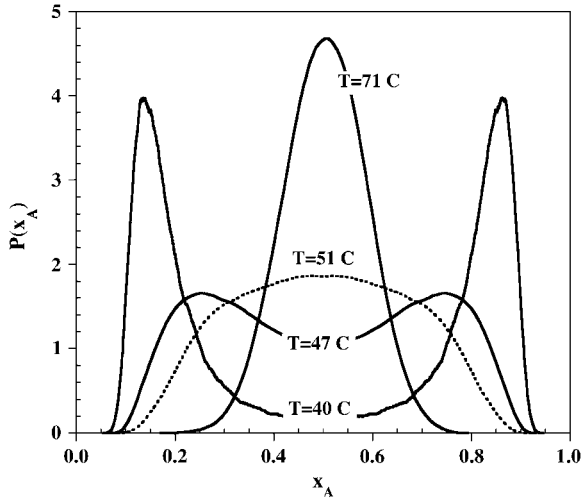

FIGURE 2 Lipid composition probability distribution functions $P(x_A)$ for $L = 50$ at the temperatures shown for a pure lipid mixture (no obstacles). Above the critical temperature, $P(x_A)$ has one peak, and below the critical temperature it has two peaks, which are located at the concentrations of the coexisting phases. At the critical temperature for this system size (*dashed curve*), $P(x_A)$ is very flat. The apparent critical temperature for this system size is $T_c = 51°C$. From finite size scaling, we determine that the true (infinite system) critical temperature is $T_c = 40°C$.

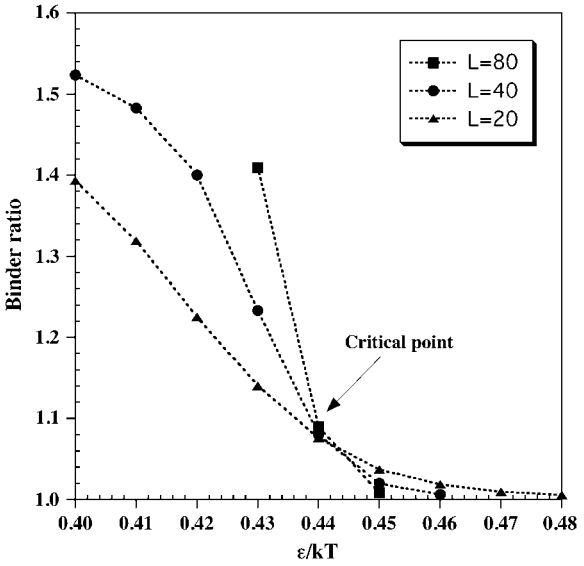

FIGURE 3 Determination of the critical temperature of the infinite systems from simulations of finite systems. The Binder ratio is plotted as a function of temperature for various system sizes. The true critical temperature is the temperature at which the Binder ratio is independent of system size, i.e., the three curves cross.

displays two symmetric peaks, indicative of the coexistence of two phases. The apparent critical temperature for $L = 50$ is 50°C.

The critical temperature is known to be a strong function of the system size, but the true (infinite system) critical temperature can be obtained from finite size scaling (24). The critical temperature of a finite system is always higher than that of the infinite system. One way to estimate the true critical temperature is to calculate the critical temperature for a number of system sizes and then extrapolate (using the finite size scaling ansatz) to the infinite system. This method is not convenient because for each system size one has to obtain (from simulations) the coexistence curve and then use a scaling analysis to obtain the critical temperature. A further analysis of the dependence of this critical temperature as a function of system size gives the true (infinite system) critical temperature.

A more convenient method for obtaining the true critical temperature is to use the fact (24) that the Binder ratio $B = \langle m^2 \rangle / \langle |m|^2 \rangle$ is independent of system size at the true critical temperature, where $m = 2x_A - 1$ is the order parameter, and $\langle A \rangle$ and $|A|$ denote, respectively, the ensemble average and absolute value of the quantity A. Fig. 3 depicts B as a function of ε/kT for three different system sizes ($L = 20$, 40, and 80) in the absence of obstacles. B is a sigmoidal curve and becomes steeper as the system size is increased. The critical temperature is the temperature at which the curves intersect. In the absence of obstacles, our result agrees with the exact result for the two-dimensional Ising model, as it should. When static obstacles are present, we calculate B for each configuration of the obstacle proteins and then average over many (10–20) such realizations. In all cases, we plot B as a function of temperature for three different system sizes ($L = 20$, 40, and 80) and determine the critical temperature from the temperature at which the curves intersect.

RESULTS AND DISCUSSION

The presence of static obstacles dramatically reduces the critical temperature. Fig. 4 depicts $P(x_A)$ for a lipid mixture in the presence of immobile obstacles at $\phi = 0.1$ for a number of temperatures. The apparent critical temperature can be estimated from the temperature at which the distribution becomes very flat (it becomes bimodal below the apparent critical temperature). For $\phi = 0.10$ the apparent critical temperature is 26°C, which can be compared to the apparent critical temperature of 51°C in the absence of obstacles (Fig. 2) for the same system size. The true (infinite system) values of T_c are 40°C and 5°C, respectively; the obstacle-induced depression of T_c is 35°C.

Fig. 5 depicts the critical temperature of the infinite system as a function of area fraction of proteins. The critical temperature is a strong function of the area fraction of the obstacle proteins, decreasing in a roughly linear fashion from 40°C to 5°C as f increases from 0 to 0.1. In fact, for $\phi > 0.1$, the obstacles decrease T_c below the freezing point of water.

The coexistence curve is the boundary between combinations of T and x_A for which a single liquid phase exists, and combinations for which two liquid phases of different composition coexist. At each temperature below T_c, the simulation yields two symmetric points on the coexistence curve

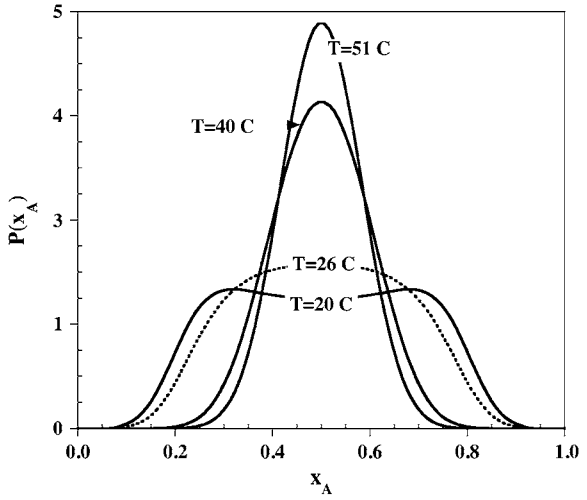

FIGURE 4 Lipid composition probability distribution functions $P(x_A)$ for $L = 50$ at the temperatures shown for a lipid mixture in the presence of obstacles at 10% by area. $P(x_A)$ at the apparent critical temperature (for this system size) is given by the dashed curve, which is for $T_c = 26°C$. The true critical temperature, obtained by finite size scaling, is $T_c = 5°C$.

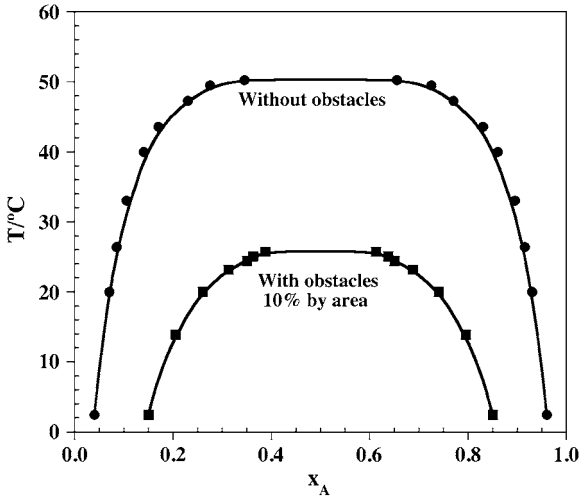

FIGURE 6 Coexistence curve of the lipid mixture for $L = 50$. Lines are meant to guide the eye.

from the values of x_A at the maxima in $P(x_A)$. Fig. 6 depicts the coexistence curves with no obstacles and with obstacles at $\phi = 0.10$ area coverage. The obstacles shift the coexistence curve downward in temperature and narrow it as well.

The formation of micrometer-sized lipid domains implies phase separation of the lipid mixture. Therefore, lipid rafts are possible only for $T < T_c$. In other words, our model system studied as a pure lipid mixture at 37°C would phase separate (form large, coexisting liquid domains). The same system studied in the presence of immobile obstacles at only 10% area coverage at the same temperature would not phase separate

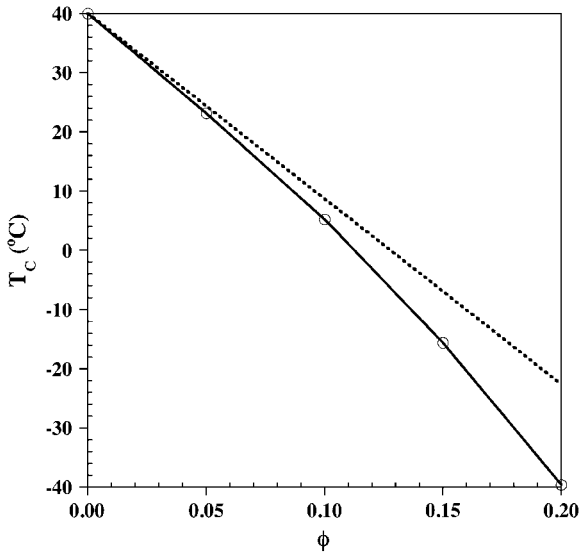

FIGURE 5 Variation of the true critical temperature with the area fraction of protein obstacles. The dashed line is the prediction of the mean-field theory described in the text.

but would exhibit nanometer-scale clusters of A and of B. This is highly reminiscent of the experimental results (13,19).

The phase transition observed for lipid mixtures in vitro is the demixing of two liquid phases. Our model is the simplest that exhibits such a transition. This new physical effect in two dimensions is reminiscent of the well-known effect of confinement (between two flat plates) on the phase behavior of a three-dimensional binary liquid (25). Such confinement also suppresses phase separation, independent of the details of the fluid-surface interactions. This can be viewed as primarily a geometric effect; confinement prevents the growth of correlations in one dimension, thereby effectively decreasing the dimensionality of space.

The effect of obstacles is very strong, and because it affects behavior on long length scales, it is likely to be independent of details of the molecular model. In fact, simple mean-field theory for the suppression of the critical temperature is consistent with the simulation results. A mean-field theory estimate for the free energy of mixing, F_{mix}, for a binary mixture on a lattice is

$$\frac{F_{mix}}{kT} = x_A \ln x_A + x_B \ln x_B + \frac{2z}{kT}\varepsilon x_A x_B, \qquad (2)$$

where z is the coordination number of the lattice. In the above, the first two terms come from the entropy of mixing, and the last term is the interaction energy of mixing and is derived by assuming that the probability of finding a lipid molecule in the lattice site next to another lipid molecule is independent of position of either molecule and only a function of the mean composition of species and coordination number of the lattice (mean-field approximation). The critical temperature is obtained by setting $(\partial^2 F_{mix})/(\partial x_A^2) = 0$, which gives $T_c = (\varepsilon z)/k$. In a crude approximation, we assume that the only effect of the obstacles is to reduce the number of possible neighbors for each lipid molecule in an average fashion, i.e., we replace z by $z(1 - \phi)$ in Eq. 2.

Because the probability of finding a site without an obstacle is $1 - \phi$, and $z = 4$, the mean-field estimate for the critical temperature is

$$T_c = \frac{4\varepsilon}{k}(1 - \phi) = (1 - \phi)T_c(\phi = 0), \quad (3)$$

where $T_c(\phi = 0)$ is the critical temperature in the absence of obstacles. The dashed line in Fig. 5 represents the mean-field theory prediction, i.e., $T_c = (1 - \phi)\, T_c(\phi = 0)$, and shows that the theory is in good agreement with simulations for the obstacle-induced depression of the critical point, at least for low values of ϕ.

The mean-field theory does not, however, predict the narrowing of the phase boundary seen in Fig. 2 because the presence of obstacles merely serves to change the effective temperature scale. This is important because it emphasizes the fact that there is a physical feature of the presence of obstacles that is not captured in a mean-field treatment of the problem.

The model can be readily generalized to include a ternary mixture whose energetics mimic those of Chol/sphingomyelin/PC mixtures (18,26), to include attractive or repulsive interactions between obstacles and lipid components, and to include mobile proteins in addition to the immobile obstacles. It would also be interesting to run time-evolved simulations to measure the size and lifetimes of the transient nanodomains.

Individual snapshots of small-scale simulations differ in ways that can be quite misleading. $P(x_A)$ is broad (Fig. 2) in part because of the finite size of the system. In this situation, there may be no such thing as a ''representative'' snapshot. Nevertheless, examination of dozens of snapshots suggests that the obstacles tend to lie on boundaries between A-rich and B-rich nanodomains (Fig. 7). This propensity could be the result of the energetic ''neutrality'' of the obstacles. It is more favorable for A-rich or B-rich domains to terminate at an obstacle or line of obstacles than at an A-B contact because there is no associated energy penalty. In this way, the mean spacing between obstacles may influence the size distribution of A-rich or B-rich lipid ''nanodomains''. In a real biological membrane, one can imagine neutral obstacle-lipid interactions, attractive obstacle-A interactions, or attractive obstacle-B interactions. We have little quantitative information about protein-lipid interaction energies to guide model building. In addition to obstacle spacing, attractive interactions between specific lipids (or Chol) and protein obstacles (or mobile membrane proteins) could also be important for regulating the size and lifetime of A-rich or B-rich nanodomains. Such attractions might also induce formation of long-lived protein-lipid domains, as has been previously suggested (27).

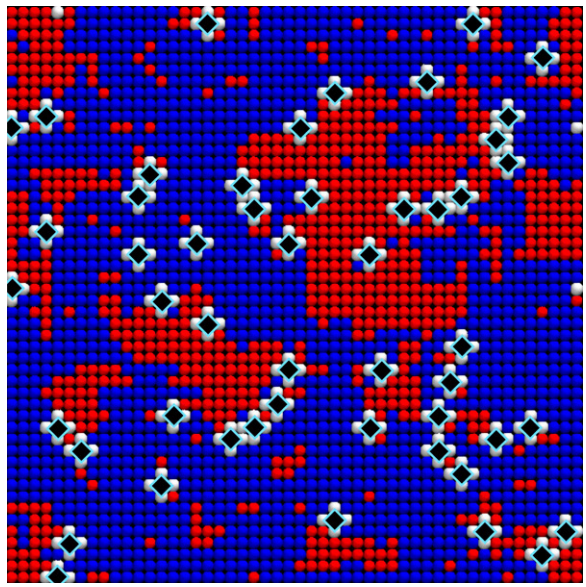

FIGURE 7 Snapshot of a simulation with $L = 50$ and $\phi = 0.1$ for $T = 37°C$, which is below T_c.

CONCLUSIONS AND OUTLOOK

We present a simple model to investigate raft formation in the plasma membrane (PM). Our main conclusion is that rafts in biological membranes could be nanoscopic rather than macroscopic. The difference between the PM and artificial membranes composed of lipid mixtures arises from the presence of proteins anchored to the cytoskeleton. These proteins act as obstacles to the lipids and suppress macroscopic phase separation. These predictions could be tested experimentally in vitro by preparing artificial membranes composed of raft-forming lipid mixtures on surfaces that contain nanometer-scale obstacles. Preliminary results with obstacles of different shapes and sizes show a suppression of the critical temperature similar to that seen in this work, and the degree of suppression is almost identical for mobile and immobile obstacles (H. Duwe III, J. C. Weisshaar, and A. Yethiraj, article in preparation).

What might be the nature of the obstacles in vivo? The observation of ''hop diffusion'' of G-protein-coupled receptors in the single-molecule tracking experiments of Kusumi and co-workers (29) provides experimental evidence for the existence of obstacles. They hypothesize that the PM consists of corrals bounded by spectrin filaments connected to junctional complexes that bind the filaments to the membrane. These complexes could play the role of the obstacles in our simple model. The corrals are typically ~30–40 nm in one dimension. A 30-nm square lattice of junctional complexes would require only 45 nm^2 of obstacle area per corral to reach $\phi = 0.05$ and significantly depress T_c. In addition to the junctional complexes themselves, very large integral membrane proteins that diffuse slowly compared with lipids could also contribute. The formation of crystalline regions induced by Chol depletion is another possible source of obstacles (30).

The present model is in qualitative accord with a wide variety of experimental data. As already noted, recent attempts

to observe clustering of GPI-APs in the PM indicate that rafts, if they exist, are nanometer-sized and transient (13). Our model is consistent with nanometer-sized rafts, although it does not address the issue of their transience. It has recently been demonstrated that PM material from rat basophilic leukemia cells can indeed phase separate into two liquid domains. The two phases were observed by lipid staining of chemically induced blebs and of giant unilamellar vesicles made from harvested bleb material (31). Phase separation was sensitive to temperature. Our interpretation is that blebs lack cytoskeletal elements that can anchor protein obstacles, which enables formation of micrometer-sized domains.

Our model does not address alternative explanations for the absence of micrometer-sized lipid rafts. Sharma et al. (13) and Plowman et al. (32) observe nanometer-sized clusters of GPI anchored proteins, but the ratio of monomers to clusters was constant for a large range of protein expression levels. They argue that this feature implies an active regulation of the clusters of proteins. Because this effect is not incorporated into our model for the membrane, we cannot say anything definitive about this issue.

We certainly do not rule out the possibility of special situations in which lipid domain formation is permitted by a paucity of protein obstacles or driven by attractive protein-lipid interactions. For example, micrometer-sized, long-lived domains in which the dye Laurdan exhibits an emission spectrum indicating a liquid-ordered (L_o) phase were observed in living RAW macrophages at 22°C (33). These domains were concentrated on filopodia, adhesion points, and cell-cell contact areas. Interestingly, the area covered by the L_o phase was temperature sensitive, decreasing from 44% at 22°C to 25% at 37°C. In the same work, fibroblasts showed no evidence of an L_o phase under the same conditions. Our conclusions are consistent with these experiments, although not enough is known about obstacles or interactions to quantitatively model them.

This work was supported by the National Science Foundation under Grant Nos. CHE-0315219 (to A.Y.) and CHE-0452375 (to J.C.W.) and by National Institutes of Health-National Institute of Neurological Disorders and Stroke under Grant No. R01NS051518 (to J.C.W.). Acknowledgment is made to the donors of the American Chemical Society Petroleum Research Fund for partial support of this research under Grant No. 42834-AC4 (to J.C.W.).

REFERENCES

1. London, E. 2005. How principles of domain formation in model membranes may explain ambiguities concerning lipid raft formation in cells. *Biochim. Biophys. Acta.* 1746:203–220.
2. Lagerholm, B. C., G. E. Weinreb, K. Jacobson, and N. L. Thompson. 2005. Detecting microdomains in intact cell membranes. *Annu. Rev. Phys. Chem.* 56:309–336.
3. Silvius, J. 2005. Lipid microdomains in model and biological membranes: how strong are the connections? *Q. Rev. Biophys.* 38:373–383.
4. Kenworthy, A. K., B. J. Nichols, C. L. Remmert, G. M. Hendrix, M. Kumar, J. Zimmerberg, and J. Lippincott-Schwartz. 2004. Dynamics of putative raft-associated proteins at the cell surface. *J. Cell Biol.* 165: 735–746.
5. Carrasco, M., M. J. Amorim, and P. Digard. 2004. Lipid raft-dependent targeting of the influenza A virus nucleoprotein to the apical plasma membrane. *Traffic.* 5:979–992.
6. Chiang, S. H., C. A. Baumann, M. Kanzaki, D. C. Thurmond, R. T. Watson, C. L. Neudauer, I. G. Macara, J. E. Pessin, and A. R. Saltiel. 2001. Insulin-stimulated GLUT4 translocation requires the CAP-dependent activation of TC10. *Nature.* 410:944–948.
7. Suzuki, N., S. Suzuki, D. G. Millar, M. Unno, H. Hara, T. Calzascia, S. Yamasaki, T. Yokosuka, N. J. Chen, A. R. Elford, J. Suzuki, A. Takeuchi, C. Mirtsos, D. Bouchard, P. S. Ohashi, W. C. Yeh, and T. Saito. 2006. A critical role for the innate immune signaling molecule IRAK-4 in T cell activation. *Science.* 311:1927–1932.
8. Palazzo, A. F., C. H. Eng, D. D. Schlaepfer, E. E. Marcantonio, and G. G. Gundersen. 2004. Localized stabilization of microtubules by integrin- and FAK-facilitated Rho signaling. *Science.* 303:836–839.
9. Kamiguchi, H. 2006. The region-specific activities of lipid rafts during axon growth and guidance. *J. Neurochem.* 98:330–335.
10. Takahashi, E., O. Inanami, T. Ohta, A. Matsuda, and M. Kuwabara. 2006. Lipid raft disruption prevents apoptosis induced by 2-chloro-2′-deoxyadenosine (Cladribine) in leukemia cell lines. *Leuk. Res.* 30: 1555–1561.
11. Hattori, C., M. Asai, H. Onishi, N. Sasagawa, Y. Hashimoto, T. C. Saido, K. Maruyama, S. Mizutani, and S. Ishiura. 2006. BACE1 interacts with lipid raft proteins. *J. Neurosci. Res.* 84:912–917.
12. Baumgart, T., S. T. Hess, and W. W. Webb. 2003. Imaging coexisting fluid domains in biomembrane models coupling curvature and line tension. *Nature.* 425:821–824.
13. Sharma, P., R. Varma, R. C. Sarasij, Ira, K. Gousset, G. Krishnamoorthy, M. Rao, and S. Mayor. 2004. Nanoscale organization of multiple GPI-anchored proteins in living cell membranes. *Cell.* 116:577–589.
14. Jacobson, K., and C. Dietrich. 1999. Looking at lipid rafts? *Trends Cell Biol.* 9:87–91.
15. Edidin, M. 2003. The state of lipid rafts: from model membranes to cells. *Annu. Rev. Biophys. Biomol. Struct.* 32:257–283.
16. Glebov, O. O., and B. J. Nichols. 2004. Distribution of lipid raft markers in live cells. *Biochem. Soc. Trans.* 32:673–675.
17. Kenworthy, A. K., and M. Edidin. 1998. Distribution of a glycosyl-phosphatidylinositol-anchored protein at the apical surface of MDCK cells examined at a resolution of $<$100 A using imaging fluorescence resonance energy transfer. *J. Cell Biol.* 142:69–84.
18. McConnell, H. 2005. Complexes in ternary cholesterol-phospholipid mixtures. *Biophys. J.* 88:L23–L25.
19. Veatch, S. L., and S. L. Keller. 2005. Miscibility phase diagrams of giant vesicles containing sphingomyelin. *Phys. Rev. Lett.* 94:148101.
20. Metropolis, N., A. W. Rosenbluth, M. N. Rosenbluth, A. H. Teller, and E. Teller. 1953. Equation of state calculations by fast computing machines. *J. Chem. Phys.* 21:1087–1092.
21. Stanley, H. E. 1971. Introduction to Phase Transitions and Critical Phenomena. Oxford Science Publications, New York.
22. Wolff, U. 1989. Collective Monte Carlo updating for spin systems. *Phys. Rev. Lett.* 62:361–364.
23. Hoshen, J., and R. Kopelman. 1976. Percolation and cluster distribution.1. Cluster multiple labeling technique and critical concentration algorithm. *Phys. Rev. B.* 14:3438–3445.
24. Landau, D. P., and K. Binder. 2000. A Guide to Monte Carlo Simulations in Statistical Physics. Cambridge University Press, Cambridge.
25. Fisher, M. E., and H. Nakanishi. 1981. Scaling theory for the criticality of fluids between plates. *J. Chem. Phys.* 75:5857–5863.
26. Feigenson, G. W., and J. T. Buboltz. 2001. Ternary phase diagram of dipalmitoyl-PC/dilauroyl-PC/cholesterol: nanoscopic domain formation driven by cholesterol. *Biophys. J.* 80:2775–2788.
27. Almeida, P. F., A. Pokorny, and A. Hinderliter. 2005. Thermodynamics of membrane domains. *Biochim. Biophys. Acta.* 1720:1–13.

28. Reference deleted in proof.

29. Suzuki, K., K. Ritchie, E. Kajikawa, T. Fujiwara, and A. Kusumi. 2005. Rapid hop diffusion of a G-protein-coupled receptor in the plasma membrane as revealed by single-molecule techniques. *Biophys. J*. 88:3659–3680.

30. Nishimura, S. Y., M. Vrljic, L. O. Klein, H. M. McConnell, and W. E. Moerner. 2006. Cholesterol depletion induces solid-like regions in the plasma membrane. *Biophys. J*. 90:927–938.

31. Baumgart, T., A. T. Hammond, P. Sengupta, S. T. Hess, D. A. Holowka, B. A. Baird, and W. W. Webb. 2007. Large-scale fluid/fluid phase separation of proteins and lipids in giant plasma membrane vesicles. *P Natl Acad Sci USA*. 104:3165–3170.

32. Plowman, S. J., C. Muncke, R. G. Parton, and J. F. Hancock. 2005. H-ras, K-ras, and inner plasma membrane raft proteins operate in nanoclusters with differential dependence on the actin cytoskeleton. *Proc. Natl. Acad. Sci. USA*. 102:15500–15505.

33. Gaus, K., E. Gratton, E. P. Kable, A. S. Jones, I. Gelissen, L. Kritharides, and W. Jessup. 2003. Visualizing lipid structure and raft domains in living cells with two-photon microscopy. *Proc. Natl. Acad. Sci. USA*. 100:15554–15559.